Far-Flow Approximations for Precursor Ionization Profiles

LEWIS WETZEL*
Brown University, Providence, R. I.

Some of the features of two far-flow models which have previously been introduced to account for the presence of precursor ionization ahead of a hypersonic shock front are examined. These models are based, respectively, on photoionization of the upstream gas by shock radiation and on the diffusion of charges from the actively ionized region. Neither model involves the active shock directly, and so their implications are useful mainly in estimating the shape of precursor ionization profiles. We concentrate chiefly on those profiles produced by shock radiation in gases whose photon absorption cross sections are decreasing functions of energy above the ionization edge. Dramatic departures from simple exponential decay are found for gases like helium, atomic hydrogen, and, to a lesser extent, argon, molecular hydrogen, and nitrogen. The average energy of the photoelectrons decays gradually until thermal equilibrium is reached far upstream. The diffusion model reduces, in the far-flow limit, to exponential decay governed by the free electron diffusion length, regardless of the nature of the space-charge fields, although these fields might produce space-charge-limited diffusion.

Introduction

WHEN considering the production of ionization by a shock wave, it is usually assumed that the ionization density is zero at the translational/rotational shock front. Since, however, the total shock structure includes the region ahead of this front, the detection of ionization in this so-called "precursor" region indicates that the foregoing assumption yields an approximation to the growth of ionization which, although often very good,[1] might also be misleading.[2] Accordingly, precursor phenomena might have important implications in an accurate understanding of total shock structure, especially in the case of strong shocks. From a more practical point of view, communication with, and identification of, a hypersonic vehicle could depend to a detectable extent upon the details of the envelope of ionization surrounding it. At most radar frequencies, the interaction of electromagnetic waves with the ionization takes place at electron densities many orders of magnitude below the electron densities at shock equilibrium, and the details of the density profiles at low relative levels, that is, in the precursor regime, therefore could be significant.

Unfortunately, the experiments in which precursor effects have been detected have been provocative rather than crucial. Most of them have been performed in shock tubes in which the problems of disentangling true shock behavior from the artifacts of shock production and probe response and structure are formidable. However, the accumulation of evidence in a wide variety of experimental situations over the past several years[2–12] leaves little doubt that ionization can appear in measurable amounts ahead of a normal shock front under certain conditions.

Although some progress has been made in identifying precursor ionization as part of the complete shock,[13] the usual procedure in attempting to understand the presence of precursor effects is to adopt a simplified model based on some selected feature of the real, active shock. In order for ionization to appear ahead of the translational/rotational front, transport of either an ionizing agency or the ions themselves must take place across this front. According to one hypothesis, recombination radiation escaping upstream from the strongly ionized gas behind the front provides such an ionizing agency. Phenomenological treatments of the production of precursor ionization by this means begin with a simple model in which the actual shock is replaced by a photon emitter directing an ionizing flux of prescribed spectral distribution against a streaming gas.[14, 15] (In the relatively complicated case of shocks in air,[14] this model has been used to interpret certain results obtained in one of the few experiments not conducted in a shock tube.[11]) A primary purpose of this paper is the elucidation of some features of the forementioned model.

Another hypothesis begins with the recognition that a sharp rise in the level of ionization behind the front will be accompanied by large density gradients in the ionic species, resulting in a strong tendency for the electrons and ions to diffuse across the front into the precursor region.[4, 5] Treatments of this problem show some variety: electron diffusion is considered as a perturbation on a shock ionization distribution calculated neglecting diffusion[16]; electron profiles in a streaming gas are considered without reference to a shock[6]; the shock is replaced by a plane electron source moving with the shock speed[17]; the shock is replaced by an actively ionized slab-like region in a streaming gas[18]; the electron and ion distributions at the interface between an ionized half-space and a vacuum are considered.[19] There is a good deal of consistency among these various treatments, and we will discuss them in greater detail later on.

Few of the models mentioned in the last two paragraphs involve the gasdynamics of the shock in any essential way. Most usually, the real shock is assumed to provide a flux of ionizing radiation or ions and electrons, and one considers the distribution of the resulting precursor ionization well upstream, the near-flow behavior being replaced by a fictitious source of some kind. It is in this sense that we call these approximations "far-flow approximations," and it is to this class of problems that we restrict our attention.

The mathematical model most often used in these approximations consists of some simplification of the one-dimensional particle and momentum transport equations for electrons and ions in the streaming gas, augmented by Poisson's equation to provide electrostatic coupling between these two charged species. (Although higher moments are usually ignored, we will have occasion to consider a phenomenological energy equation in a later section.) A

Presented as Preprint 63-457 at the AIAA Conference on Physics of Entry into Planetary Atmospheres, Cambridge, Mass., August 26–28, 1963; revision received April 7, 1964. This work was sponsored by the Advanced Research Projects Agency (Ballistic Missile Defense Office) and technically administered by the Fluid Dynamics Branch of the Office of Naval Research. I would like to thank W. Prager for the computer program leading to Fig. 2 and C. M. Angulo for a useful discussion on the behavior of certain integrals. The remarks of one of the reviewers of this paper were especially helpful.

* Associate Professor of Engineering.

typical set of such equations has been reduced in Ref. 18 to the following three:

$$D_e \frac{\partial^2 n_e}{\partial x^2} + \mu_e \frac{\partial}{\partial x}(En_e) + u \frac{\partial n_e}{\partial x} = -q(x) \quad (1)$$

$$D_i \frac{\partial^2 n_i}{\partial x^2} - \mu_i \frac{\partial}{\partial x}(En_i) + u \frac{\partial n_i}{\partial x} = -q(x) \quad (2)$$

$$\epsilon_0(\partial E/\partial x) = e(n_i - n_e) \quad (3)$$

where n_e and n_i are the electron and ion densities, and D_e, μ_e and D_i, μ_i are the respective diffusion and mobility coefficients relative to the neutral flow. E is the electrostatic field, u the flow velocity, and $q(x)$ a source function. [For completeness, a sink function $s(x)$ should be added to the right side of (2) and (3) to allow for volume losses from, say, recombination. Under most shock conditions of interest, such losses are unimportant in the precursor region, and so we will ignore them from the start.] The one-dimensional shock-based coordinate system is shown in Fig. 1.

Precursor Ionization Due to Shock Radiation

In the equilibrium region, well behind an ionizing shock front in a homogeneous gas, ionization and deionization processes must be in balance. A radiant flux will be associated with the deionization processes (freebound transitions), and some of this flux can be expected to escape into the region ahead of the shock front, producing photoionization of the cold gas. Properly, of course, this flux contributes an additional mechanism for energy transfer and should be included in the basic equations describing the total shock structure.[12, 13] However, lacking a clear understanding of the role of radiative transfer in shock problems, we will assume in what follows that a radiative flux with spectral distribution $P(\nu)$, ν being the frequency, is directed upstream from the shock front into the cold streaming gas; for the flow velocities and types of gases usually under consideration, recombination in the upstream region may be ignored, and so there will be no returning flux. Referring to Fig. 1, this model is equivalent to placing a photon emitter, characterized by $P(\nu)$, in the plane $x = 0$.

Profile Calculation

In order to concentrate on precursor profiles due solely to photoionization of the gas ahead of the shock, we will ignore not only the sink function $s(x)$, but also the first two terms on the left side of both (1) and (2), leaving them in the form

$$-u(\partial n/\partial x) = q(x) \quad (4)$$

with no distinction now being possible between the electron and ion distributions. If $q(x)$ is due to photoionization, then when ν is greater than the ionization frequency ν_i, we may introduce a partial source function $q(x;\ \nu)d\nu$ giving the number of ionizations per unit volume per second produced by photons in the range of frequencies from ν to $\nu + d\nu$. We will now associate a partial ionization density $n(x;\ \nu)d\nu$ with each range of photon frequencies, where the two incremental functions are related to the total source and density functions by

$$q(x) = \int_{\nu_i}^{\infty} q(x;\ \nu)d\nu \quad (5)$$

and

$$n(x) = \int_{\nu_i}^{\infty} n(x;\ \nu)d\nu \quad (6)$$

Inserting these expressions into (4) and assuming uniform convergence of the integrals, we may solve for $n(x;\ \nu)$ from

$$-u[\partial n(x;\ \nu)/\partial x] = q(x;\ \nu) \quad (7)$$

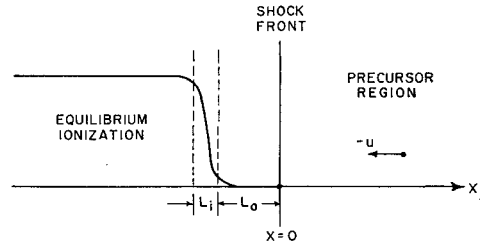

Fig. 1 Shock coordinate system and some characteristic lengths.

It will be convenient to replace the radiation flux density $P(\nu)$ by a photon flux density $N(\nu) = P(\nu)/h\nu$, giving the number of photons per unit area per second per unit frequency range emerging from the emitter at $x = 0$. The probability that a photon of frequency ν will penetrate the gas to a distance x and be absorbed between x and $x + dx$ is just $n_a Q_a(\nu) \exp[-n_a Q_a(\nu)x]dx$, where n_a is the number density of the gas particles in the precursor region, and $Q_a(\nu)$ is the absorption cross section for photons of frequency ν in that gas. Furthermore, the provisional probability that an absorbed photon will produce an ionization may be written as $Q_i(\nu)/Q_a(\nu)$, with $Q_i(\nu)$ the ionization cross section for photons of frequency ν. Therefore, the partial source function becomes

$$q(x;\ \nu) = n_a Q_i(\nu) \exp[-n_a Q_a(\nu)x]N(\nu) \quad (8)$$

Substituting into (11) and solving for $n(x;\ \nu)$, we get

$$n(x;\ \nu) = [Q_i(\nu)/uQ_a(\nu)] \exp[-n_a Q_a(\nu)x]N(\nu) \quad (9)$$

and inserting this into (10), the total ionization density $n(x)$ becomes

$$n(x) = u^{-1} \int_{\nu_i}^{\infty} N(\nu) \exp[-n_a Q_a(\nu)x]d\nu \quad (10)$$

where we have made an initial simplification by assuming that $Q_i(\nu) = Q_a(\nu)$. This is reasonable in the absence of competing absorption processes like photodissociation. The exponent in the integrand of (14) can be expressed in terms of dimensionless quantities by writing

$$n_a Q_a(\nu)x = [Q_a(\nu)/Q_a(\nu_i)]x/[n_a Q_a(\nu_i)]^{-1} = f(\nu)\eta \quad (11)$$

where $f(\nu) = Q_a(\nu)/Q_a(\nu_i)$ is the absorption cross section normalized with respect to its value at the ionization edge [we will refer to $f(\nu)$ as the "absorption profile"], and $\eta = x/\lambda_i$ is a dimensionless distance upstream of the emitter, measured in units of a photon mean free path at the ionization edge defined by $\lambda_i = [n_a Q_a(\nu_i)]^{-1}$. Using this notation, (10) takes the simple form

$$n(\eta) = u^{-1} \int_{\nu_i}^{\infty} N(\nu) \exp[-f(\nu)\eta]d\nu \quad (12)$$

General Profile Behavior

It is possible to make some general statements about these precursor profiles without knowing the exact form of either $N(\nu)$ or $f(\nu)$. First let us look at the behavior of $\log n(\eta)$. If $f(\nu) = 1$, which would be the case for constant absorption cross section above the ionization edge, then $\log n(\eta) = \text{constant} - \eta$. The constant determines the magnitude of the precursor ionization and is very difficult to estimate with any confidence. It can be eliminated, without losing information about the shape of the precursor profile, by taking the derivative of $\log n$ with respect to η. Performing this differentiation in (12), we get

$$[\log n(\eta)]' = -\frac{\int_{\nu_i}^{\infty} N(\nu)f(\nu) \exp[-f(\nu)\eta]d\nu}{\int_{\nu_i}^{\infty} N(\nu) \exp[-f(\nu)\eta]d\nu} \quad (13)$$

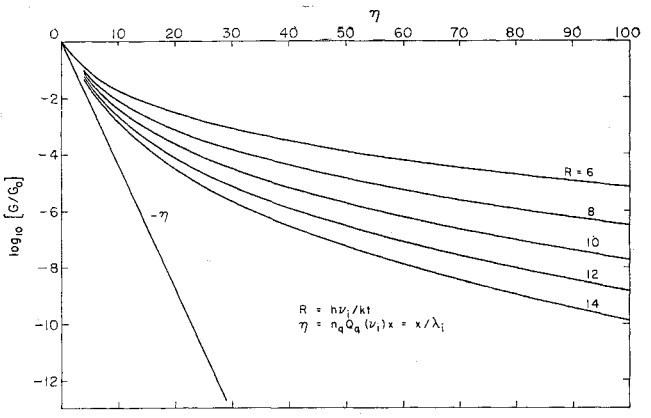

Fig. 2 Precursor ionization profiles for $f(\nu) = (\nu/\nu_i)^{-3}$; (He, H).

The right side is just the average of the absorption profile $f(\nu)$ over the partial precursor density given in (9). We see that, if f is a decreasing function for $\nu > \nu_i$, then the right side of (13) will always be less than unity; that is, the effective decay length of the precursor distribution in the neighborhood of a point $x = \lambda_i\eta$ ahead of the emitter is greater than the photon mean free path at the ionization edge. The curvature of $\log n$ is found from the second derivative, and if one differentiates (13) again, one gets

$$[\log n(\eta)]'' = \frac{\int_{\nu i}^{\infty} N(\nu)f^2(\nu)\exp[-f\eta]d\nu}{\int_{\nu i}^{\infty} N(\nu)\exp[-f\eta]d\nu} - \left[\frac{\int_{\nu i}^{\infty} N(\nu)f(\nu)\exp[-f\eta]d\nu}{\int_{\nu i}^{\infty} N(\nu)\exp[-f\eta]d\nu}\right]^2 \tag{14}$$

In a manner analogous to the proof of the Schwartz inequality by reduction to the series definition of a Riemann integral,[21] one can show that, if a weighting function $W(\nu) \geq 0$ for all ν, then

$$\int f^2(\nu)W(\nu)d\nu \int W(\nu)d\nu \geq \left[\int f(\nu)W(\nu)d\nu\right]^2 \tag{15}$$

where the equality holds when $f(\nu)$ is unity. Applying this result to (14), it is seen that the curvature of $\log n$ will always be positive. Thus, for gases characterized by decreasing $f(\nu)$, the local decay length will not only be greater than λ_i but might also be a continuously increasing function of η.

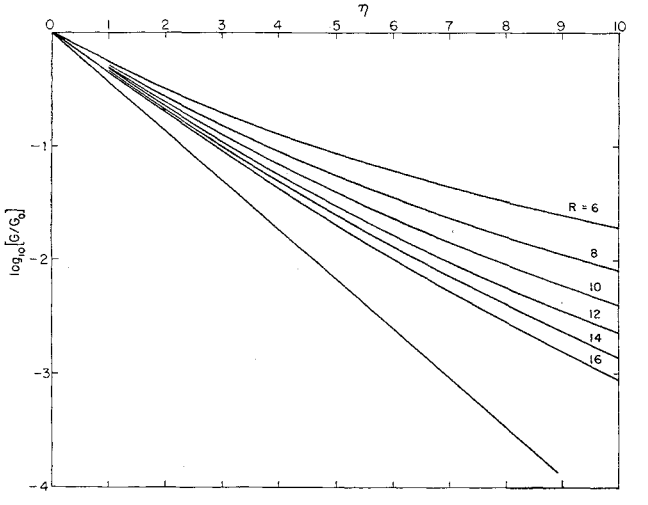

Fig. 3. Detail of Fig. 2 for $0 \leq \eta \leq 10$.

Specific Example

The particular form to be chosen for the photon distribution at the emitter will depend upon the optical thickness of the shocked gas for ionizing photons. At these high energies, however, the photon distribution is dominated by the Boltzmann factor $\exp[-h\nu/kT]$, whatever the optical thickness, and we will find that the far-flow profile shapes will be completely determined by this factor. For illustrative purposes, we will choose the distribution characteristic of a blackbody at temperature T in the high-energy limit; that is,

$$N(\nu) = (2\pi/c^2)\nu^2\exp[-h\nu/kT] \qquad \nu \geq \nu_i \gg kT/h \tag{16}$$

For a radiating shock in a homogeneous gas, this expression not only overestimates the magnitude of the photon flux but also neglects discontinuities in the range $\nu > \nu_i$ due to recombination into both ground and excited states of multiply ionized atoms in the actively ionized region behind the front. In all but very strong shocks, however, the population of multiply ionized atoms will be small, and so, for the sake of simplicity, we will ignore effects associated with multiple ionizations in both upstream and downstream regions.

The absorption profile $f(\nu)$ differs widely from one gas to another and is generally given as an empirical function.[22] In some gases, $f(\nu)$ remains relatively constant over a large range of energies above the ionization edge, by which we will always mean the first ionization frequency for an atom or molecule in its ground state. Very rough examples of such gases might be neon or molecular oxygen, whose precursor profiles should be closely exponential. We are, however, primarily interested here in functions $f(\nu)$ that decrease rapidly with increasing $\nu > \nu_i$. The most extreme examples of this behavior are provided by helium and atomic hydrogen, whose absorption cross sections are given very closely by Kramer's formula[22]:

$$Q_a(\nu) = Q_a(\nu_i)(\nu/\nu_i)^{-3} \tag{17}$$

making the absorption profile

$$f(\nu) = (\nu/\nu_i)^{-3} \tag{18}$$

This is the case that we will examine in some detail below. Certain other gases, like argon and molecular hydrogen and nitrogen, also have absorption cross sections that fall quite rapidly beginning with values of $h\nu$ a few volts above $h\nu_i$. We will touch on them very briefly.

In order to explore the implications of (16) and (18), let us substitute the indicated expressions for $N(\nu)$ and $f(\nu)$ into (12), yielding

$$n(\eta) = u^{-1}\left(\frac{2\pi}{c^2}\right)\int_{\nu_i}^{\infty} d\nu\nu^2\exp\left[\frac{-h\nu}{kT} - \eta\left(\frac{\nu}{\nu_i}\right)^{-3}\right] \tag{19}$$

Introducing a new variable of integration $\mu = (\nu/\nu_i) - 1$ and a dimensionless parameter $R = h\nu_i/kT$, we may write (19) in the form

$$n(\eta) = u^{-1}\left(\frac{2\pi}{c^2}\right)\nu_i^3 e^{-R}\int_0^{\infty} du(1+\mu)^2\exp[-R\mu - \eta(1+\mu)^{-3}] \tag{20}$$

Defining

$$G(\eta;\ R) = \int_0^{\infty} d\mu(1+\mu)^2\exp[-R\mu - \eta(1+\mu)^{-3}] \tag{21}$$

and calling $G(0;\ R) = G_0(R)$, we reduce (20) to the compact form

$$n(\eta) = n(0)[G(\eta;\ R)/G_0(R)] \tag{22}$$

where the expression in brackets completely describes the behavior of the precursor ionization profile. The function $G(\eta;\ R)$ was computed by the Brown University IBM 7070 computer, using a quadrature subroutine, for the values $R = 6, 8, 10, 12, 14$ and $\eta = 0, 1, 2, 4, 6, 8, 10, 12, 20, 40, 60, 80, 100$. The corresponding precursor profiles $\log(G/G_0)$

are plotted in Fig. 2. The details of the behavior of small η between 0 and 10 are plotted separately in Fig. 3. It is obvious that the effect of falling cross sections can be quite dramatic.

Two characteristic features of the precursor profiles are evident from these curves. First, the decay length is increased directly ahead of the emitter and is a function of emitter temperature. Second, the local decay length appears to be a monotonically increasing function of distance as one moves away from the emitter, and the positive curvature of $\log(G/G_0)$ is evident. Both of these results are to be expected on the basis of the general expressions for slope and curvature given in (13–15).

The effective decay length at the emitter is found by letting $\eta \to 0$ in (13). This is just the average of $f(\nu)$ over the initial photon distribution, the actual decay length being found by dividing into λ_i. It is easy to show that, if $N(\nu)$ is given by (16) and $f(\nu)$ by (18), the result is approximately

$$[\log n(\eta)]'_{\eta=0} \simeq -(1 - 1/R + 2/R^2)/(1 + 2/R + 2/R^2) \quad (23)$$

This expression almost exactly reproduces the computed behavior of $\log n$ shown in Fig. 3 for values of η close to the emitter.

Far-Flow Behavior of Precursor Profiles

The asymptotic behavior of the precursor profiles for large η can be found under fairly general conditions. For shocks of any optical thickness, we may assume that $N(\nu)$ has the form

$$N(\nu) = g(\nu) \exp[-h\nu/kT] \qquad \nu \geq \nu_i \quad (24)$$

where $g(\nu)$ varies slowly with ν as compared with the exponential factor. Equation (13) then takes the form

$$[\log n(\eta)]' = -\frac{\int_{\nu_i}^{\infty} f(\nu) \exp\left[\frac{-h\nu}{kT} - f(\nu)\eta\right] g(\nu)d\nu}{\int_{\nu_i}^{\infty} \exp\left[\frac{-h\nu}{kT} - f(\nu)\eta\right] g(\eta)d\nu} \quad (25)$$

Both integrands are dominated by the same exponential, whose argument is $-A(\nu) = -R(\nu/\nu_i) - f(\nu)\eta$. If η is sufficiently large and $f(\nu)$ decreases rapidly above the ionization edge, this argument can have a maximum for some value of ν above ν_i. The major contributions to the two integrals will then arise from values of ν in the neighborhood of this maximum. The location of this point, if it exists, is found by setting

$$\frac{\partial A(\nu)}{\partial(\nu/\nu_i)} = R + \nu_i \frac{\partial f(\nu)}{\partial \nu} \eta = 0 \quad (26)$$

and, when possible, solving for ν_m from $f'(\nu_m) = -R/\nu_i\eta$. For absorption profiles $f(\nu)$ that permit a solution to (26), an approximation to (25) can be obtained by expanding $A(\nu)$ in a power series about ν_m and evaluating the two integrals in the sense of a saddle-point integration. The calculation is straightforward, and if only the dominant term is retained, the result is equivalent to replacing the right side of (25) by the value of f at the maximum ν_m; that is,

$$[\log n(\eta)]' \approx -f(\nu_m) \qquad \eta \text{ large} \quad (27)$$

When $f(\nu) = (\nu/\nu_i)^{-3}$, the value of (ν_m/ν_i), satisfying (26), is found to be

$$(\nu_m/\nu_i) = (3\eta/R)^{1/4} \qquad 3\eta > R \quad (28)$$

Substituting this into (27), we find

$$[\log n(\eta)]' \approx -(R/3\eta)^{3/4} \quad (29)$$

whose integral may be written as

$$\log n(\eta) \approx -4(R/3)^{3/4}\eta^{1/4} + C(R) \quad (30)$$

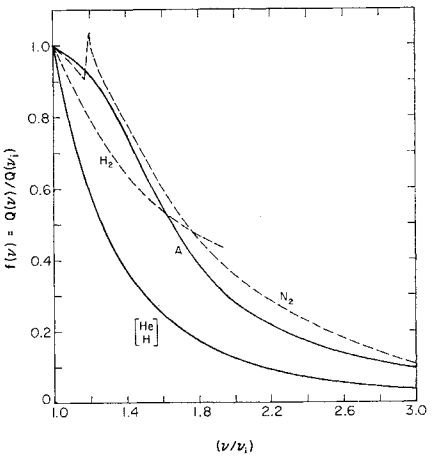

Fig. 4 Normalized absorption cross sections for He, H, A, H_2, and N_2.

Comparison with the computed curves in Fig. 2 shows that $C(R) \propto R^{3/4}$ and that the far-flow behavior can be fairly well approximated by

$$\log n(\eta) \approx -R^{3/4}[(\eta/3)^{1/4} - 1] \qquad \eta > 20 \quad (31)$$

Any gas whose absorption cross section falls with sufficient rapidity should experience a similar lifting of the far-flow precursor profile. In Fig. 4 we have plotted the absorption profiles $f(\nu) = Q_a(\nu)/Q_a(\nu_i)$ for several such gases, using the data in Ref. 23. (For the molecular gases H_2 and N_2, the empirical behavior is not sharp at the first ionization edge, and so we have defined $\nu/\nu_i = 1$ at the first maximum of the ionization cross section, which appears a little above the indicated first ionization frequency.) In the case of argon, the decrease of $f(\nu)$ for $(\nu/\nu_i) > 1.5$ appears to resemble that of the helium and atomic hydrogen, that is, to decrease like $(\nu/\nu_i)^{-3}$. [A closer check shows that, for $(\nu/\nu_i) > 1.5$, $f(\nu) \sim (\nu/\nu_i)^{-2.8}$.] The solutions of (26) for argon and helium should be very similar, therefore, and the far-flow precursor profiles described through (27) should also be similar for the two gases. In order to verify this inference, as well as to provide an accurate picture of precursor profiles for a gas much used in experiments, a numerical integration of $G(\eta; R)$ was performed (by hand this time) using the empirical values of $f(\nu)$ for argon found in Fig. 4. The resulting profiles are shown in Fig. 5, where the helium profile for $R = 10$ is included for reference.

Approximate analytical expressions for the *shape* of the precursor profiles for H_2 and N_2 can easily be obtained from

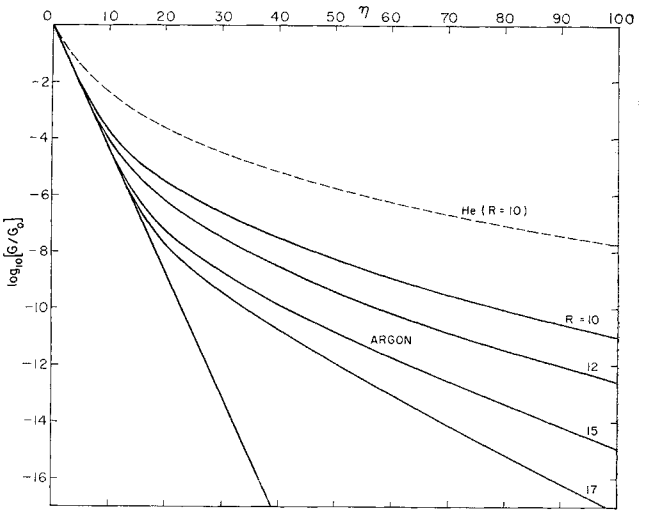

Fig. 5 Precursor profiles for argon [$f(\nu)$ empirical].

(26) and (27). From Fig. 4 one finds that over most of the range of (ν/ν_i) the absorption profiles are given approximately by $f(\nu) \sim (\nu/\nu_i)^{-1}$ for H_2 and by $f(\nu) \sim (\nu/\nu_i)^{-2}$ for N_2. Rough estimates of the shapes of the precursor profiles in the far-flow region are found to be

$$\log n(\eta) \approx -3(R/2)^{2/3}\eta^{1/3} + C_N(R) \quad \text{for} \quad N_2 \qquad (32)$$

and

$$\log n(\eta) \approx -2R^{1/2}\eta^{1/2} + C_H(R) \quad \text{for} \quad H_2 \qquad (33)$$

These show a more rapid decrease of $\log n$, corresponding to the smaller penetration of high-energy photons into the streaming gas.

Average Energy of the Precursor Photoelectrons

In order to find the average energy of the precursor electrons, we consider the balance between heating of the electrons by the excess energy left over after ionization and the loss of energy through both convection and cooling collisions with the neutral gas. If we assume that all of the energy in excess of the ionization energy $h\nu_i$ is carried away by the departing electron, then the rate at which energy is being delivered to the photoelectrons at x may be written, using (8) and (11), as

$$W = \int_{\nu_i}^{\infty} h(\nu - \nu_i)q(x;\ \nu)d\nu$$
$$= \lambda_i^{-1}\int_{\nu_i}^{\infty} h(\nu - \nu_i)f(\nu)\exp[-f(\nu)\eta]N(\nu)d\nu \qquad (34)$$

On the other hand, if $n(\eta)$ is the electron density at η, and $U(\eta)$ is the average electron energy, then the average energy density at η is $n(\eta)U(\eta)$, and the energy loss by convection is $-u\partial(nU)/\lambda_i\partial\eta$. Moreover, if electrons of energy U are in collisional interaction at the rate ν_c with heavy particles of average energy U_0 (in this case $U_0 = \frac{3}{2}kT_0$, where T_0 is the upstream temperature of the streaming gas), then the usual expression for the average energy loss rate per unit volume is

$$\delta\nu_c n(\eta)[U(\eta) - U_0] \qquad (35)$$

where δ is the energy loss parameter ($\delta = 2m/M$ for elastic collisions between electrons of mass m and heavy particles of mass M). A phenomenological energy equation can therefore be written in the form

$$-(u/\lambda_i)[n(\eta)U(\eta)]' + \delta\nu_c n(\eta)[U(\eta) - U_0] = W(\eta) \qquad (36)$$

A simple approximation to this equation may be found by ignoring the convection term. The average energy then becomes

$$U(\eta) \approx U_0 + (1/\delta\nu_c)W(\eta)/n(\eta) \qquad (37)$$

(The collision frequency ν_c is usually a function of U, but we will assume it to be a constant in this approximation.) The ratio W/n is just (u/λ_i) times the average of $h(\nu - \nu_i)f(\nu)$ over the precursor density at η, as can be seen by substituting from (34) and (12). Using the relation $\nu_c = v_t/\lambda_m$, where λ_m is the mean free path for collisions between electrons of thermal velocity v_t and the heavy particles, (37) may be written as

$$U(\eta) \approx U_0 + [u\lambda_m/\delta v_t\lambda_i]h\nu_i\langle(\nu/\nu_i - 1)f(\nu)\rangle|_\eta \qquad (38)$$

For a typical helium shock with $u \sim 3 \times 10^6$ cm/sec, the forementioned coefficient in brackets is close to unity. In the limit of large η, the average can be calculated using the method described in the last section, and we obtain for this case

$$U(\eta) \approx U_0 + h\nu_i[(R/3\eta)^{1/2} - (R/3\eta)^{3/4}] \qquad \eta \gg 1 \qquad (39)$$

As $\eta \to \infty$, the average photoelectron energy approaches the average energy of the unshocked gas, as it should. The rate at which U decreases with η in (39) is quite slow, and it is therefore easy to show that for large η the convection term in (36) is smaller than the dissipation term, and, therefore, that (39) is a reasonable approximation to the average photoelectron energy in the far-flow limit.

Precursor Profiles from Electron Diffusion

If the source terms on the right sides of (1) and (2) are neglected, the remaining equations, augmented by (3), describe electron and ion profiles as they are established by a balance between upstream currents driven by concentration gradients and electrostatic forces and the convection of charges back toward the shock front with the streaming gas. Discussions of the diffusion hypothesis for precursor effects generally have their basis in some simplification of this set of equations. Several experiments[3, 6, 9] indicate the presence of electrons alone in the precursor region, and so, in the simplest model, the ion equation (2) is ignored altogether; that is, one sets $n_i = 0$. The electric self-field of the electron distribution may now also be ignored,[17] or it may be included.[6, 18, 24] If E and q are set equal to zero in (1), the resulting equation is easily solved to give[17]

$$\log n_e(x) = -x/L_e + C \qquad (40)$$

where

$$L_e = D_e/u \qquad D_e = kT_e/m\nu_c \qquad (41)$$

The characteristic length L_e is a diffusion length for electrons in the streaming gas, where D_e is the diffusion coefficient for free electrons. It is a relatively simple matter to include the electrostatic self-field of the electrons alone. Since $n_i = 0$, n_e may be substituted from (3) into (1), resulting in a nonlinear equation for E in standard form, whose solution allows n_e to be recovered through (3). Both Weymann[6] and Pipkin[17] give similar solutions for n_e, the former being

$$n_e(x) = \frac{2kT_e\epsilon_0}{e^2L_e^2}\,\frac{A(A-1)\exp(-x/L_e)}{[A-(A-1)\exp(-x/L_e)]^2} \qquad (42)$$

(rationalized mks units). The constant A is to be determined from initial conditions, and if $n_e(0) = n_0$, it is easily found that $A \approx L_e/2^{1/2}L_{D0}$, where $L_{D0} = (kT_e\epsilon_0/e^2n_0)^{1/2}$ is the debye length for the initial density. For any experimental situation of possible interest, $L_{D0} \ll L_e$.

An interesting and rather important observation may be made upon examining the solution (42) more closely. In the limit of small $x \ll L_e$, (42) may be approximated by

$$n_e(x) \approx \frac{n_0}{(1 + x/2^{1/2}L_{D0})^2} \qquad (x \ll L_e) \qquad (43)$$

For an intermediate range of x between L_{D0} and L_e, (43) becomes

$$n_e(x) \approx \frac{2kT_e\epsilon_0}{e^2L_e^2}\,\frac{1}{(x/L_e)^2} \qquad (L_{D0} \ll x \ll L_e) \qquad (44)$$

whereas for $x > L_e$ we get

$$n_e(x) \approx \frac{2kT_e\epsilon_0}{e^2L_e^2}\exp\left(\frac{-x}{L_e}\right) \qquad x > L_e \qquad (45)$$

which is the same profile as given in (40) for pure diffusion. From (44) and (45) one sees that, when x is greater than the local debye length at the origin, the precursor distribution no longer depends upon the initial density, n_0 being a function only of local parameters like T_e and u. It is of interest to note that the result expressed in (44) is exactly the same as the equilibrium electron distribution obtained by Langmuir[25] in studying space-charge-limited flow in a vacuum diode in which the plate is removed to infinity. In this

case, $L_e = \infty$, and it was noted that the distribution of electrons ahead of a thermionic emitter is independent of the maximum current available, that is, of the material and characteristics of the emitter. Equation (43) was also found by Abele[19] for the electron distribution in a vacuum adjacent to a stable ionized half-space, although he did not seem to appreciate the implications of making $x > L_{D0}$. Finally, starting with an equation equivalent to (42), Pipkin[18] considered the limit as $L_e \to \infty$ and obtained (44) as representing the maximum precursor distribution that could be expected.

The conclusion we draw here is that, in the model for pure electron diffusion, the initial value n_0 affects the distribution only in a small region within about one debye length of the "front." Between a debye length L_{D0} and an electron diffusion length L_e, the distribution resembles that resulting from space-charge limiting of the electron distribution in a vacuum. For distances greater than L_e, the far-flow distribution is governed by free electron diffusion in the streaming gas and is given by (45). Calculating the coefficient of the exponential for a case of possible interest in which $T_e = 10^4$ °K, $L_e = 3$ cm, we find

$$n_e(x) \approx 10^5 \exp(-x/L_e)\text{cm}^{-3} \qquad x > L_e \qquad (46)$$

which is probably too small even to be measured by the conventional probes used in shock tubes.

When ions are included, the distance over which electron-ion coupling may be considered important is given by the ambipolar diffusion length $L_a = D_a/u$, where $D_a \ll D_e$, and so $L_a \ll L_e$. This implies that the pure electron model in which $n_i = 0$ would have some relation to reality in any shock, and that the crucial region of space-charge-limited behavior described by (44) should generally exist within the first electron diffusion length L_e past the "front," which is now considered to be the very narrow region over which the diffusion is essentially ambipolar.

If the preceding inferences are true, there is little point in pursuing the diffusion hypothesis any further, at least in the realm of far-flow precursor approximations. One would still expect diffusion of the ambipolar type to occur in the near-flow region, governed by a diffusion length much smaller than L_e (which is more or less verified in Ref. 4). Moreover, since space-charge limiting is suggested on the basis of one-dimensional electrostatics, the possibility remains that the precursor electrons in the three-dimensional geometry of certain small bore shock tubes might depart significantly from the behavior appropriate for a one-dimensional shock.[5, 24] The proper interpretation of experiments on precursor effects in shock tubes will require an accurate understanding of this problem.

Discussion and Conclusions

A point of interest in any far-flow approximation is the way in which it might fit local conditions in the near-flow region. In the cases discussed here, this region is immediately ahead of the main body of active ionization, where the two models each presume that some kind of initial photon distribution or electron density may be definitely prescribed at a transverse reference plane $x = 0$. The normal rate processes describing the growth of ionization behind a shock front cannot produce an instantaneous jump in ionization at the shock front. If this were the case, our results could be viewed as second-order effects derived from the first-order behavior, in the sense that Bond considered electron diffusion in an argon shock.[15]

This situation may be clarified a bit by considering two further characteristic lengths: an "onset length" L_0 that measures the distance behind the front before the ionization begins to grow rapidly toward some equilibrium level, and an "ionization length" L_i that is a measure of the width of the region over which this rapid growth takes place. These lengths are illustrated in Fig. 1. When L_0 and L_i are much smaller than any of the characteristic lengths of the approximations, like λ_i or L_e, the approximations might be expected to give a reasonable representation of the distribution of ionization over the precursor region. If L_0 becomes appreciable while L_i remains small, then one must take into account the discontinuity in the density of the neutral gas at the front. The reference plane $x = 0$ is moved back to the ionization discontinuity ($L_i \sim 0$), and the "precursor region" of the modified model contains a discontinuity in λ_i (via n_a) or L_e (via ν_c, T, and u) at the front. This means that the scale of the near-flow behavior in the far-flow approximations is reduced by a factor of $\frac{1}{4}$ to $\frac{1}{10}$ or so. The photoionization model can probably be applied to this case by suitable interpretation of the dimensionless parameter η. Finally, when L_i approaches λ_i or L_e, it is clear that the far-flow behavior of the model is part of the over-all shock behavior, and the distribution of ionization in the precursor region can no longer be plausibly decoupled from the basic shock structure. Theoretically, of course, one cannot know L_i or L_0 without first knowing the effects of photoionization and charge diffusion on the structure of the shock, and so these far-flow approximations might be useful as an aid in understanding certain empirical results but must be considered heuristic at best.

References

[1] Lin, S. C. and Teare, J. D., "Rate of ionization behind shock waves in air. II. Theoretical interpretations," Phys. Fluids **6**, 355–375 (1963).

[2] McLean, E. A., Faneuff, C. E., Kolb, A. C., and Griem, H. R., "Spectroscopic study of helium plasmas produced by magnetically driven shock," Phys. Fluids **3**, 843–856 (1960).

[3] Hollyer, R. N., Jr., "Preliminary studies in the APL high temperature shock tube," Johns Hopkins Univ., Applied Physics Lab., Rept. CM-903 (May 1957).

[4] Groenig, H., "Measurements of diffusion of electrons out of strong shock waves," Inst. fver Mechanik, Technical Univ., Aachen, Final Rept. on Contract AF 61(514)-1046 (June 1959).

[5] Weymann, H. D., "Electron diffusion ahead of shock waves in argon," Phys. Fluids **4**, 545–548 (1960).

[6] Weymann, H. D. and Troy, B., "Electron and ion density profiles ahead of shock waves in argon," Bull. Am. Phys. Soc. **6**, 212 (1961).

[7] Gloersen, P., "Some unexpected results of shock-heating xenon," Phys. Fluids **3**, 857–870 (1960).

[8] Jones, D. L., "Precursor electrons ahead of cylindrical shock waves," Phys. Fluids **5**, 1121–1122 (1962).

[9] Groenig, H., "Precursor photoionization and electrons," Phys. Fluids **6**, 142–144 (1963).

[10] Camm, J., Kivel, B., Taylor, R. L., and Teare, J. D., "Absolute intensity of non-equilibrium radiation in air and stagnation heating at high altitudes," J. Quant. Spectry. Radiative Transfer *2*, 509–514 (1962).

[11] Lin, S. C., "Radio echoes from a manned satellite during re-entry," J. Geophys. Res. **67**, 3851–3870 (1962).

[12] Zivanovic, S., "Investigation of precursor ionization in front of the shock waves of hypersonic projectiles," AIAA Preprint 63-458 (August 26–28, 1963).

[13] Ferrari, C. and Clarke, J. H., "Photoionization upstream of a strong shock wave," Brown Univ., Div. of Engineering, Rept. Cm-1020 (January 1963).

[14] Hammerling, P., "Ionization effects of precursor radiation from shocks in air," Avco-Everett Research Lab. Rept. 98 (June 1960).

[15] Wetzel, L., "A feature of precursor ionization profiles due to shock radiation," Phys. Fluids **6**, 750–752 (1963).

[16] Bond, J. W., Jr., "Plasma physics and hypersonic flight," Jet Propulsion **28**, 228–235 (1958).

[17] Wetzel, L., "Precursor effects and electron diffusion from a shock front," Phys. Fluids **5**, 827–830 (1962).

[18] Pipkin, A. C., "Diffusion from a slightly ionized region in a uniform flow," Phys. Fluids **4**, 1298–1302 (1961).

[19] Abele, M., "Electron distribution across a discontinuity of ion density in a plasma," Polytechnic Inst. of Brooklyn Rept. 549 (March 1960).

[20] Goulard, R., "Fundamental equations of radiation gas dynamics," AGARD Fluid Dynamics Panel Meeting, High Temperature Aspects of Hypersonic Flow, Rhode Saint Genese, Belgium (April 1952).
[21] Bohm, D., *Quantum Theory* (Prentice-Hall, Inc., New York, 1951), Chap. 10.
[22] Bates, D. R. (ed.), *Atomic and Molecular Processes* (Academic Press, New York, 1962), Chap. 3.
[23] Weissler, G. L., *Handbuch der Physik* (Springer-Verlag, Berlin, 1956), Vol. XXI, pp. 304–342.
[24] Pipkin, A. C., "Precursor waves in shock tubes," Phys. Fluids **6**, 1382–1388 (1963).
[25] Langmuir, I., "The effect of space charge and initial velocities on the potential distribution and thermionic current between parallel plane electrodes," Phys. Rev. **21**, 419–435 (1923).

JULY 1964 AIAA JOURNAL VOL. 2, NO. 7

A Quasi-One-Dimensional Treatment of Chemical Reactions in Turbulent Wakes of Hypersonic Objects

S. C. LIN* AND J. E. HAYES†
Avco-Everett Research Laboratory, Everett, Mass.

The effects of different mixing models on the chemical reaction histories in the turbulent wakes of hypersonic objects are investigated in a quasi-one-dimensional approximation. The radial propagation of the turbulent front is represented as a prescribed entrainment boundary and the chemical composition of the initial flow entering the boundary is calculated according to existing approximate methods for tracing chemical reactions in laminar flows. In the absence of a suitable chemical kinetics theory for turbulent flows, only the limiting cases of extremely slow and extremely fast viscous dissipation are considered for the subsequent turbulent mixing process. Specific examples are presented for the flow behind hypersonic spheres in air. In the slow-dissipation case, the high-entropy gas in the wake remains hot, and may even be reheated strongly by three-body atomic recombination. This gives rise to large amplitude fluctuations of the chemical species. In the fast dissipation case, the temperature generally falls off rapidly with distance behind the sphere, but moderately strong reheating may still take place due to sudden enhancement of the exothermic exchange reaction $N + O_2 \rightarrow NO + O$. The mean electron density in the far wake is found to be extremely sensitive to the mixing model.

I. Introduction

THE study of wake phenomena behind high-speed objects in the earth's atmosphere has stimulated considerable interest in hypersonics research in recent years.[1] In 1959, Feldman[2] obtained a set of numerical solutions for the conduction-controlled laminar trails behind spheres at hypersonic speeds, using a quasi-equilibrium equation of state for the high-temperature air throughout the flow field. However, from an earlier estimate, by one of the authors,[3] of the characteristic chemical and ionization relaxation times for the various parts of the flow field, it was found that the high-entropy wake[4] would always be out of chemical equilibrium except at gas densities corresponding to hypersonic flight at relatively low altitudes. In view of the fact that the wake behind objects of ordinary sizes would become turbulent at low altitudes, the assumptions of laminar flow and of local chemical equilibrium did not appear to be mutually compatible. This, indeed, has been found to be the case from more detailed calculations of the streamwise relaxation histories[5] and from recent experimental studies of the wake transition phenomenon.[6–10]

The theoretical problem of turbulent diffusion in the wake of a blunt-nosed body at hypersonic speeds was first treated by Lees and Hromas[11] in 1961, adopting Reynolds hypothesis of similarity between the turbulent transfer of mass, momentum and energy, and using a turbulent diffusivity extrapolated from Townsend's low-speed experiments. In order to bring out the main fluid dynamics effects without undue complications by rate processes, Lees and Hromas again assumed the equation of state of the gas to be that corresponding to local thermodynamic equilibrium everywhere in the flow field. This treatment has also been extended to wakes behind slender hypersonic objects, such as hemisphere cones and pure cones.[12] Although the calculated rate of growth of the turbulent wake appeared to agree well with experimental observations, predictions of the thermal and chemical properties of the wake from such theoretical models remain of doubtful value until the question of reaction rates in the flow field is properly examined.

More recently, various authors[13–15] have proposed to use the integral method[4] for simultaneous treatment of diffusion and chemical relaxation in turbulent as well as laminar wakes behind objects of arbitrary (but axisymmetric) shape. The terms for production (or depletion) of chemical species in the species conservation equations in these treatments are

Presented as Preprint 63-449 at the AIAA Conference on Physics of Entry into Planetary Atmospheres, Cambridge, Mass., August 26–28, 1963; revision received April 27, 1964. This work was supported jointly by Headquarters, Ballistic Systems Division, Air Force Systems Command, U. S. Air Force, under Contract No. AF 04(694)-33 and Advanced Research Projects Agency monitored by Army Missile Command, U. S. Army, under Contract No. DA-19-020-AMC-0210 as part of Project Defender. The authors wish to acknowledge the help and encouragement from many of their colleagues at the Avco-Everett Research Laboratory during the course of this work. They wish to thank especially J. D. Teare for his invaluable advice, and G. J. Dreiss for his able assistance in carrying out the computer program required for the numerical calculations.

* Principal Research Scientist. Associate Fellow Member AIAA.
† Principal Research Scientist.